Spin Currents in Diluted Magnetic Semiconductors

S. D. Ganichev,[1] S. A. Tarasenko,[2] V. V. Bel'kov,[2] P. Olbrich,[1] W. Eder,[1] D. R. Yakovlev,[2,3] V. Kolkovsky,[4] W. Zaleszczyk,[4] G. Karczewski,[4] T. Wojtowicz,[4] and D. Weiss[1]

[1]*Terahertz Center, University of Regensburg, 93040 Regensburg, Germany*
[2]*A. F. Ioffe Physico-Technical Institute, Russian Academy of Sciences, 194021 St. Petersburg, Russia*
[3]*Experimental Physics 2, TU Dortmund University, 44221 Dortmund, Germany*
[4]*Institute of Physics, Polish Academy of Sciences, 02-668 Warsaw, Poland*

(Received 12 December 2008; published 16 April 2009)

We study zero-bias spin separation in (Cd, Mn)Te/(Cd, Mg)Te diluted magnetic semiconductor structures. The spin current generated by electron gas heating under terahertz radiation is converted into a net electric current by applying an external magnetic field. The experiments show that the spin polarization of the magnetic ion system enhances drastically the conversion process due to giant Zeeman splitting of the conduction band and spin-dependent electron scattering on localized Mn^{2+} ions.

DOI: 10.1103/PhysRevLett.102.156602 PACS numbers: 72.25.Fe, 73.21.Fg, 73.63.Hs, 78.67.De

The generation of spin currents in low-dimensional semiconductor structures has recently attracted a lot of interest. A pure spin current is formed by directly opposed and equal flows of spin-up and spin-down electrons. While the net electrical current is zero, the spin current is finite and leads to a spatial spin separation. As a consequence, up and down spins pile up at opposing edges of the sample. Spin currents in semiconductors can be generated by electric fields, like in the spin Hall effect [1,2], or optically by employing interband transitions in noncentrosymmetric materials [3–5]. Alternatively, they can be achieved as a result of zero-bias spin separation, e.g., by electron gas heating followed by spin-dependent energy relaxation of carriers [6]. In low-dimensional semiconductor structures, pure spin currents have been reported so far only for nonmagnetic materials. However, spin-dependent effects can be greatly enhanced due to exchange interaction between electrons and magnetic ions in diluted magnetic semiconductors (DMSs) [1,7–9]. Moreover, the strength of these effects can be widely tuned by temperature, magnetic field, and concentration of the magnetic ions.

Here we report on the observation of zero-bias spin separation in (Cd, Mn)Te/(Cd, Mg)Te DMS quantum wells (QWs). We show that the free carrier absorption of terahertz (THz) radiation causes a pure spin current flow. The effect is probed in an external magnetic field which converts the spin current into a net electric current. This conversion in DMSs is greatly enhanced compared to nonmagnetic structures. The application of an external magnetic field results not only in a giant Zeeman spin splitting of the conduction band but evokes also spin-dependent exchange interaction between electrons and magnetic impurities. Both effects destroy the cancellation of spin-up and spin-down electron flows yielding a net electric current. We demonstrate that spin-dependent exchange scattering of electrons by magnetic impurities plays an important role in current generation, providing yet another handle to manipulate spin-polarized currents.

We study spin currents in (Cd, Mn)Te/(Cd, Mg)Te single QW structures grown by molecular-beam epitaxy on (001)-oriented GaAs substrates [10–12]. Evenly spaced $Cd_{1-x}Mn_xTe$ thin layers were inserted during the growth of 10 nm wide QW [Fig. 1(a)] applying the digital alloy technique [13]. Two DMS samples were fabricated: sample *A* containing two layers of three-monolayer-thick

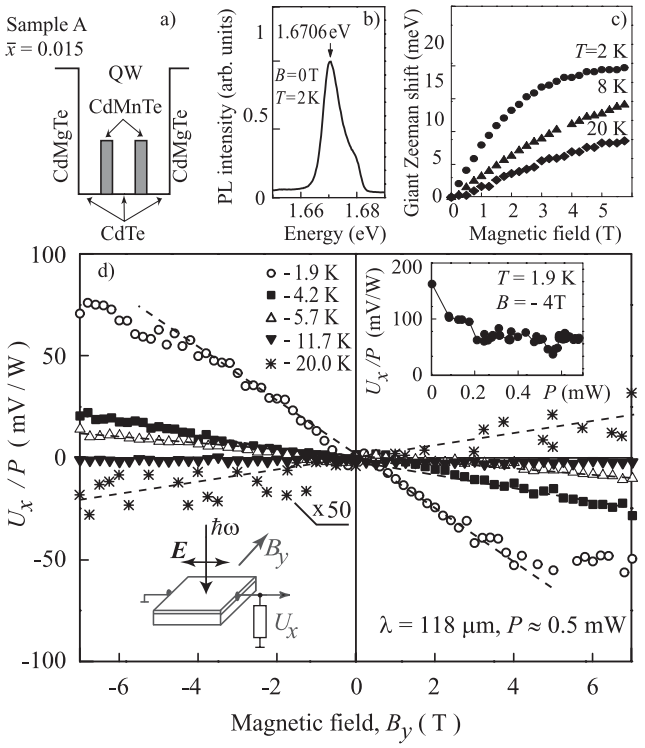

FIG. 1. Sample *A*: (a) Sketch of the structure. (b) Photoluminescence spectrum. (c) Shift of the PL line corresponding to 1/2 of the total giant Zeeman splitting. (d) Magnetic field dependence of the signal in response to a low excitation power. The insets show U_x/P as a function of P and the experimental geometry, with radiation electric field $\boldsymbol{E} \parallel x$ and $\boldsymbol{B} \parallel y$.

$Cd_{0.8}Mn_{0.2}Te$ and sample B with three single monolayers of $Cd_{0.86}Mn_{0.14}Te$. The samples were modulation doped with iodine donors introduced into the top $Cd_{0.76}Mg_{0.24}Te$ barrier at 15 nm distance from the QW. As a reference structure, we use sample C without Mn insertion. A pair of Ohmic contacts along the direction $x \parallel [1\bar{1}0]$ were prepared [Fig. 1(d), inset]. The photoluminescence (PL) spectrum of sample A is shown in Fig. 1(b). The linewidth of 11 meV corresponds to the Fermi energy E_F [14]. In an external magnetic field, this line shows a strong spectral shift toward low energies, reflecting the giant Zeeman splitting of the band [8]. This shift, shown in Fig. 1(c), is strongly temperature-dependent and about 2.5 times larger than the giant Zeeman splitting of the conduction band states. The sample parameters are summarized in Table I.

To generate spin photocurrents, we applied low power radiation, modulated at 255 Hz, of a CH_3OH laser operating at wavelength $\lambda = 118$ μm and with a power $P \approx 0.5$ mW at the sample. Additionally, we used a high power pulsed NH_3 laser operating at $\lambda = 148$ μm and $P \approx 40$ kW [15]. THz photons with energies $\hbar\omega \approx 10$ meV were chosen to induce free carrier absorption only. The geometry of the experiment is sketched in Fig. 1(d). The photocurrent is measured across a 1 MΩ and, for pulsed radiation, across a 50 Ω load resistor.

The signal U_x of sample A under low power excitation is shown as a function of the in-plane magnetic field B_y in Fig. 1(d). The signal polarity reverses with the change of the magnetic field direction. The data were taken at temperatures between 1.9 and 20 K. A central observation is that cooling of the sample changes the signal sign and increases its absolute values by more than 2 orders of magnitude. While at moderate temperatures the signal depends linearly on B_y, at the lowest temperature of 1.9 K the photocurrent saturates at high B_y. Similar results have been obtained for sample B, displayed in Fig. 2(a). Both temperature and magnetic field dependences are typical for the magnetization of DMSs and are controlled by the exchange interaction of electrons with Mn^{2+} ions. A well-known effect of the exchange interaction is the giant Zeeman splitting [8], also detected in our samples by PL measurements [Fig. 1(c)]. The electron spin splitting in (Cd,Mn)Te is given by [8,13]

$$E_Z = g_e \mu_B B + \bar{x} S_0 N_0 \alpha B_{5/2}\left(\frac{5\mu_B g_{\mathrm{Mn}} B}{2k_B(T_{\mathrm{Mn}} + T_0)}\right), \quad (1)$$

where k_B is the Boltzmann constant and μ_B the Bohr magneton. The first term describes intrinsic spin splitting with the electron g factor $g_e = -1.64$ [16]. The second term is due to electron exchange with the Mn^{2+} ions, $g_{\mathrm{Mn}} = 2$ is the Mn g factor, and T_{Mn} is the Mn-spin system temperature. Parameters S_0 and T_0 account for the Mn-Mn antiferromagnetic interaction, and $\bar{x}$ is the effective average concentration of Mn. $B_{5/2}(\xi)$ is the modified Brillouin function, and $N_0\alpha = 220$ meV is the exchange integral for conduction band electrons. Equation (1) describes a strong temperature dependence of the Zeeman splitting which reverses its sign upon temperature variation due to opposite signs of g_e and $N_0\alpha$. This explains the sign inversion of the photocurrent: The photocurrent at $T = 22$ K and at low T flows in opposite directions [Fig. 1(d)]. However, while the sign inversion of the photocurrent takes place already at $T = 20$ K, the sign of the Zeeman splitting, detected by PL, changes at higher temperatures $T \approx 40$ K. This difference we ascribe to the heating of the Mn^{2+} spin system above the lattice temperature, an effect reported in Ref. [17]. To check this assumption, we studied the power dependence of the signal.

The increase of the radiation power results in the decrease of the normalized signal [Fig. 1(d), inset], indicating a reduction of the exchange enhanced spin splitting due to increased T_{Mn}. To amplify this effect, we applied the radiation of a higher power pulsed laser. The data obtained under low and high power excitations are compared in Fig. 2 for sample B. While under low excitation, displayed in Fig. 2(a), the signal depends strongly on temperature,

TABLE I. Sample parameters. The effective average concentration of Mn $\bar{x}$ is estimated from the giant Zeeman shift of the interband emission line [Fig. 1(c)]. Mobility μ and electron sheet density n_e data are obtained at 4.2 K in the dark.

Sample	x	$\bar{x}$	μ, cm^2/Vs	n_e, cm^{-2}	E_F, meV
A	0.20	0.015	9500	4.7×10^{11}	11.7
B	0.14	0.013	16 000	6.2×10^{11}	15.4
C	0	0	59 000	4.2×10^{11}	10.4

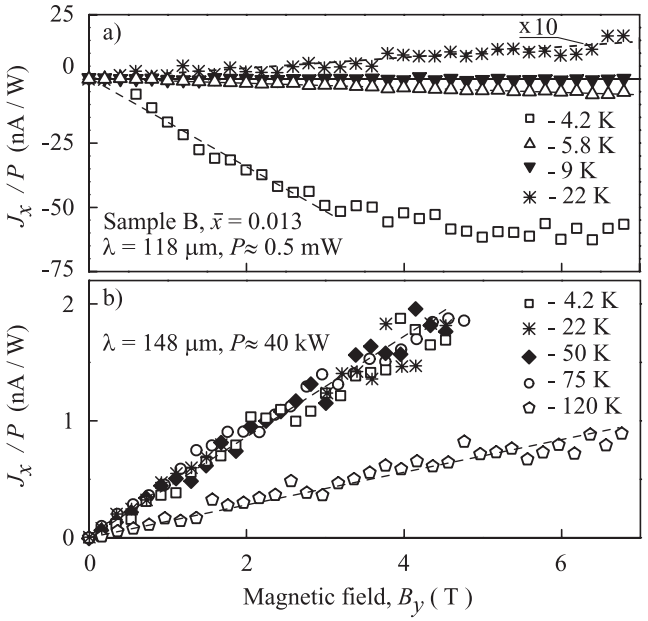

FIG. 2. Magnetic field dependence of the photocurrent J_x normalized by the radiation power P measured in sample B. (a) Low power excitation. (b) High power excitation [18].

the sign change of the photocurrent and the strong temperature dependence disappear under high excitation [Fig. 2(b)]. The T dependence under pulsed excitation is shown in Fig. 3. For $T < 100$ K the photocurrent becomes almost independent of the sample temperature, but it decreases with rising T at higher temperatures. The signal-to-noise ratio in our pulse measurements is substantially higher than that at low power. As a result, we obtain measurable signals at higher T as well as in the reference nonmagnetic sample C (Fig. 3). Remarkably, under high power excitation the absolute values and the temperature dependences of the photocurrent in DMS sample B and the reference sample C are nearly the same. This indicates that the polarization of the Mn^{2+} spins does not contribute to the current under high power excitation. We also note that the temperature dependence exposed in Fig. 3 is similar to that reported for nonmagnetic structures [6].

We now turn to microscopic mechanisms responsible for photocurrent generation. In the case of Drude absorption, photocurrents stem from spin-dependent asymmetry of the optical transitions accompanied by scattering and/or from energy relaxation [6]. Here we focus on the latter mechanism. While energy relaxation is usually considered to be spin-independent, the spin-orbit interaction in gyrotropic media, like CdTe-based QWs, adds asymmetric terms to the matrix element of electron-phonon interaction. These terms are proportional to $\sigma_\alpha(k_\beta + k'_\beta)$, where σ_α are the Pauli spin matrices and $\boldsymbol{k}$ and $\boldsymbol{k}'$ are the initial and scattered electron wave vectors, respectively. Therefore, energy relaxation processes become spin-dependent. This is indicated in Fig. 4 by bent arrows of different thickness. The asymmetry of the electron-phonon interaction results in oppositely directed electron fluxes in the spin subbands $\boldsymbol{i}_{\pm 1/2}$. The flows are of equal strength, but the total charge current is zero. Nevertheless, a finite pure spin current $\boldsymbol{J}_s = (\boldsymbol{i}_{+1/2} - \boldsymbol{i}_{-1/2})/2$ is generated resulting in a spatial spin separation [6].

The application of an external magnetic field unbalances the fluxes $\boldsymbol{i}_{\pm 1/2}$, giving rise to a net electric current $\boldsymbol{j} = e(\boldsymbol{i}_{+1/2} + \boldsymbol{i}_{-1/2})$, where e is the electron charge [6]. The obvious reason for the imbalance, also relevant for nonmagnetic semiconductors, is the Zeeman splitting of the spin subbands, sketched in Fig. 4. The fluxes $\boldsymbol{i}_{\pm 1/2}$ depend on the free carrier densities in the spin subbands $n_{\pm 1/2}$. Therefore, in a Zeeman spin-polarized system, where $n_{+1/2} \neq n_{-1/2}$, the fluxes $\boldsymbol{i}_{\pm 1/2}$ no longer compensate each other, yielding a net electric current. In DMSs, the electron Zeeman splitting is vastly enhanced due to exchange interaction between free electrons and Mn^{2+} ions. In the case of low electron spin polarization, the equilibrium electron spin per electron is given by $s = -E_Z/(4\bar{E})$, and the charge current j_Z is given by

$$\boldsymbol{j}_Z = -4e\frac{E_Z}{4\bar{E}}\left(n_e\frac{\partial \boldsymbol{J}_s}{\partial n_e}\right), \tag{2}$$

where $\bar{E}$ is an electron energy, equal to E_F for the degenerated electron gas and k_BT for the nondegenerated gas (see [19]). The spin current is written here as a function of the carrier density n_e. For Boltzmann statistics, where $\boldsymbol{J}_s \propto n_e$ and $n_e\partial \boldsymbol{J}_s/\partial n_e = \boldsymbol{J}_s$, Eq. (2) yields

$$\boldsymbol{j}_Z = -e\frac{E_Z}{k_BT}\boldsymbol{J}_s. \tag{3}$$

For the Fermi distribution, $\partial \boldsymbol{J}_s/\partial n_e$ vanishes if the spin current is solely caused by $\boldsymbol{k}$-linear terms in the matrix element of the electron-phonon interaction but is nonzero if higher order $\boldsymbol{k}$ terms contribute to the spin current.

Equation (2), showing that $j_Z \propto E_Z$, explains together with Eq. (1) the most striking experimental results: the reversal of the photocurrent direction with decreasing temperature. At high T the last term in Eq. (1) vanishes, and the

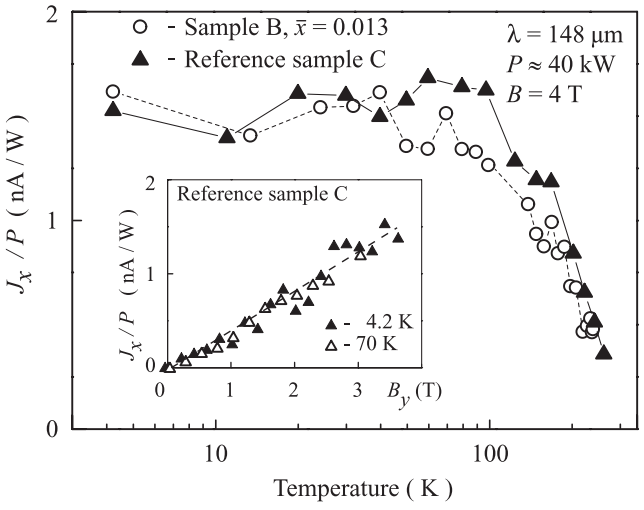

FIG. 3. Temperature dependence of J_x/P obtained at high excitation power. Results are plotted for the DMS sample B and the reference sample C. The inset shows the magnetic field dependence of the photocurrent for sample C.

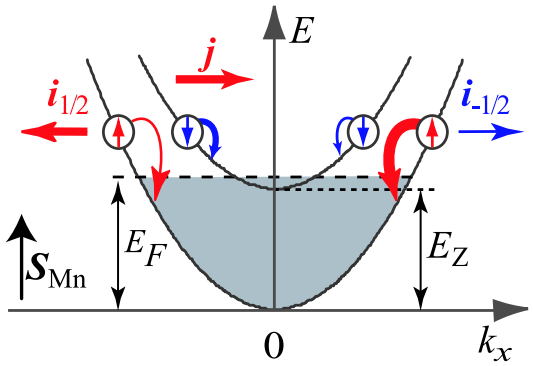

FIG. 4 (color online). Model of zero-bias spin separation and magnetic field-induced spin photocurrent. The separation is caused by scattering-assisted electron energy relaxation. Because of asymmetric relaxation, transitions to positive and negative k'_x states occur with different probabilities as indicated by bent arrows of different thickness. Electron and Mn spins are shown by arrows.

intrinsic Zeeman splitting determines the positive slope of the photocurrents in Figs. 1(d) and 2. With decreasing T the exchange term, having the opposite sign, takes over and reverses the sign of spin splitting and the direction of the photocurrent. The interplay between intrinsic and exchange contributions also results in the current inversion with rising radiation power which is caused by the heating of the Mn-spin system.

While this scenario explains qualitatively the experimental observation, it cannot explain the results quantitatively. The increase of the current strength due to the exchange enhanced E_Z in DMSs is not sufficient to explain the experimentally observed elevated current level. For sample B at $B = 3$ T, e.g., the spin splitting, derived from PL data, increases from -0.25 meV (intrinsic value given by $g_e \mu_B B$) to 2.6 meV at 4.2 K and hence by a factor of about 10. However, the magnitude of the exchange photocurrent at $T = 4.2$ K is about 40 times larger than that of the intrinsic one obtained for $T = 22$ K (see Fig. 2) [18]. Therefore, the giant Zeeman splitting can only partly explain the high photocurrents in DMSs. The additional current contribution we ascribe to the well-known spin-dependent electron scattering by polarized Mn spins [8]. This photocurrent mechanism is specific for DMSs. In an external magnetic field, when Mn spins get polarized, the scattering rates of spin-up and spin-down electrons become different [11]. This results in two different momentum relaxation times $\tau_{p,+1/2}$ and $\tau_{p,-1/2}$ in the spin subbands. Since the electron fluxes $\boldsymbol{i}_{\pm 1/2}$ are proportional to $\tau_{p,\pm 1/2}$, the polarization of Mn spins leads to an extra electric current contribution, denoted by $\boldsymbol{j}_{\mathrm{Sc}}$ below. To obtain $\boldsymbol{j}_{\mathrm{Sc}}$ theoretically, we assume that momentum relaxation of electrons is governed by their interaction with Mn^{2+} ions, localized in the QW. The corresponding Hamiltonian [8] is given by

$$H_{e-\mathrm{Mn}} = \sum_i [u - \alpha(\boldsymbol{S}_i \cdot \boldsymbol{\sigma})]\delta(\boldsymbol{r} - \boldsymbol{R}_i), \tag{4}$$

where i is the Mn ion index, $\boldsymbol{S}_i$ the vector composed of the matrices of the angular momentum 5/2, $u\delta(\boldsymbol{r} - \boldsymbol{R}_i)$ the scattering potential without exchange interaction, $\boldsymbol{r}$ the electron coordinate, and $\boldsymbol{R}_i$ the Mn ion position. The electron scattering by the Mn potential, characterized by u, is usually stronger than the exchange scattering described by α. Note that the parameter α in Eq. (4) is also responsible for the giant Zeeman splitting in Eq. (1). Then, for the case of $|\alpha| \ll |u|$, we derive

$$\boldsymbol{j}_{\mathrm{Sc}} = 4e\frac{\alpha}{u}\boldsymbol{J}_s S_{\mathrm{Mn}}, \tag{5}$$

where S_{Mn} is the average Mn spin along $\boldsymbol{B}$ (see [19]).

At low temperatures when DMS properties determine the photocurrent, both $\boldsymbol{j}_{\mathrm{Sc}}$ and $\boldsymbol{j}_Z$ have the same direction because the average electron spin caused by the giant Zeeman effect is parallel to $\boldsymbol{S}_{\mathrm{Mn}}$. The photocurrent is then given by the sum of both contributions $\boldsymbol{j} = \boldsymbol{j}_Z + \boldsymbol{j}_{\mathrm{Sc}}$. In the case of a fully spin-polarized electron gas due to the Zeeman effect, which in DMSs can be achieved at not very high magnetic fields, the electron flow in one of the spin subbands vanishes. Therefore, the electric current becomes independent of the magnetic field strength and carrier statistics and is given by $\boldsymbol{j} = \mp 2e\boldsymbol{J}_s$, where $\mp$ corresponds to $\pm$ sign of the Zeeman splitting.

In summary, electron gas heating in low-dimensional diluted magnetic semiconductors generates pure spin currents, yielding the zero-bias spin separation. We show experimentally and theoretically that the carrier exchange interaction with localized magnetic spins in DMSs vastly amplifies the conversion of a spin current into an electrical current. Two mechanisms are responsible for that: giant Zeeman splitting of the conduction band states and spin-dependent carrier scattering from localized Mn^{2+} spins polarized by an external magnetic field. In a degenerate electron gas at weak magnetic fields, the scattering mechanism dominates the current conversion.

We thank L. V. Litvin, E. L. Ivchenko, L. E. Golub, S. N. Danilov, N. S. Averkiev, and Yu. G. Semenov. The support of DFG (SFB 689), RFBR, Foundation for Polish Science, and Polish Ministry of Science is acknowledged.

[1] *Spin Physics in Semiconductors*, edited by M. I. Dyakonov (Springer, Berlin, 2008).
[2] J. Fabian *et al.*, Acta Phys. Slovaca **57**, 565 (2007).
[3] R. D. R. Bhat *et al.*, Phys. Rev. Lett. **94**, 096603 (2005).
[4] S. A. Tarasenko and E. L. Ivchenko, JETP Lett. **81**, 231 (2005).
[5] H. Zhao *et al.*, Phys. Rev. B **72**, 201302 (2005).
[6] S. D. Ganichev *et al.*, Nature Phys. **2**, 609 (2006).
[7] T. Dietl, in *Handbook on Semiconductors*, edited by T. S. Moss (North-Holland, Amsterdam, 1994), Vol. 3b.
[8] J. K. Furdyna, J. Appl. Phys. **64**, R29 (1988).
[9] C. Gorini *et al.*, Phys. Rev. B **78**, 125327 (2008).
[10] S. A. Crooker *et al.*, Phys. Rev. Lett. **75**, 505 (1995).
[11] J. C. Egues and J. W. Wilkins, Phys. Rev. B **58**, R16 012 (1998).
[12] J. Jaroszynski *et al.*, Phys. Rev. Lett. **89**, 266802 (2002).
[13] M. K. Kneip *et al.*, Appl. Phys. Lett. **88**, 152105 (2006).
[14] D. Keller *et al.*, Phys. Rev. B **72**, 235306 (2005).
[15] S. D. Ganichev and W. Prettl, *Intense Terahertz Excitation of Semiconductors* (Oxford University Press, New York, 2006).
[16] A. A. Sirenko *et al.*, Phys. Rev. B **56**, 2114 (1997).
[17] D. Keller *et al.*, Phys. Rev. B **65**, 035313 (2001).
[18] We note the fact that the slopes of $J_x(B)$ dependences in Fig. 2 detected for $T \approx 20$ K are the same for low and high power excitations indicating that the photocurrent in both cases is due to the intrinsic effect only.
[19] S. D. Ganichev *et al.*, arXiv:0811.4327.